Chapter 9
Modeling Climate Change Impacts on Stream Temperature of Formosan Landlocked Salmon Habitat

Ching-Pin Tung[1], Tsung-Yu Lee[2], and Yi-Chen Yang[3]

Abstract

This research provides a physics-based model for predicting the impact of climate change on stream temperature and in turn on Formosan Landlocked Salmon (*Oncorhynchus masou formosanus*) habitat. Because upstream watersheds in Taiwan Island are surrounded with high and steep mountains, the influence of mountain shading on solar radiation and longwave radiation is taken into account by using a Digital Elevation Model (DEM). Projections using CGCM2 and HADCM3 models and CCCM and GISS models provided information on future climatic conditions. The results indicate that annual average stream temperatures may rise by 0.5^{o}C (HADCM3 Short-term) to 2.9 ^{o}C (CGCM2 Long-term) due to climate change. The simulation results also indicate an average suitable habitat for Formosan Landlocked Salmon may decline by 333m (HADCM3 Short-term) to 1633m (CGCM2 Long-term) and 166m (HADCM3 Short-term) to 1833m (CGCM2 Long-term) depending on which thermal criterion of 17 ^{o}C or 18 ^{o}C, respectively, is applied. The results of this study draw attention to the tasks of Formosan Landlocked Salmon conservation agencies, which not only restoration plans of local environment but also mitigation strategies to global climate change are necessary and desire further research.

Keywords: Global warming, Ecology, Ecohydrology, Simulation, Modeling

9.1 INTRODUCTION

Formosan Landlocked Salmon (*Oncorhynchus masou formosanus*) is a land-locked species and currently only exists in upstream tributaries of the TaChia creek (Figure 9.1). It is the salmon that can be found in the lowest latitude in the world, but it is becoming endangered due to development of hydraulic structures and land conversion from forest to agriculture. Many efforts have been undertaken to restore the habitat of Formosan Landlocked Salmon. Formosan Landlocked Salmon is very sensitive to stream temperature. The suitable stream temperature is between 9~17 ^{o}C (Tseng, 1999), and 12 ^{o}C is the threshold during the spawning period. According to recent surveys (during 1985~1997), the isotherm of 12 ^{o}C has moved upstream by 1.56 km (Tseng, 1997). On the other hand, stream temperature higher than 17 ^{o}C has been observed in some locations during the summer.

[1] Associate Professor, Department of Bioenvironmental Systems Engineering, National Taiwan University, Taiwan. Tel:+886-2-2362-0327, Fax:+886-2-2363-5854, email: cptung@ntu.edu.tw

[2] Research Assistant, Research Center for Environmental Changes, Academia Sinica, Taiwan

[3] Research Assistant, Department of Bioenvironmental Systems Engineering, National Taiwan University, Taiwan

Global warming due to increases in greenhouse gas concentrations has attracted much attention. IPCC (2001) suggested that air temperature could increase by 1.4~5.8 ^{o}C. Stream temperature is strongly related to air temperature, and thus global warming may also threaten the habitat of Formosan Landlocked Salmon.

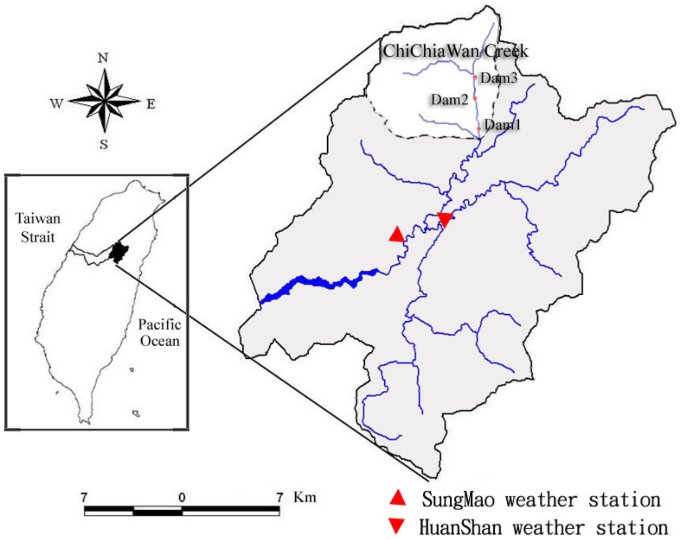

Figure 9.1 Taiwan Salmon's Habitat – upstream of the TaChia creek.

Many studies of stream temperature have been undertaken. Brown (1969, 1970a, b) estimated hourly stream temperature based on energy balance, and concluded that solar radiation is a major component and tree cover along riversides may significantly influence the amount of incident radiation. Leblanc et al. (1997) proposed a physics-based model to evaluate the effects of land use on stream temperature. Their study identified three key factors, including transmissivity and shadow area of tree cover along riversides, groundwater, and width of the river surface. Stefan and Preud'homme (1993) developed a relationship between air temperature and stream temperature, which concluded that hourly or daily water temperatures will respond to the change of air temperature. Mohseni et al. (1999) also developed a model to describe the relationships between air and stream temperatures. Stefan and Sinokrot (1993) projected stream temperature increases, given a doubling of CO_2 concentration. The results showed how stream temperature would rise under four future climate scenarios. Sinokrot and Stefan (1995) applied the stream temperature model to assess the impacts of climate change on suitable stream habitats. According to the critical stream temperature for different fish species, changes of stream length with suitable fish habitat were estimated. The study concluded that suitable habitat would be lost and the impact would be more serious for cool-water species.

The purpose of this study is to develop a physics-based model to evaluate the impacts of climate change on stream temperature in Formosan Landlocked Salmon habitat. Steep mountains are found in the upstream portion of most drainage basins in Taiwan. The shading by mountains may also play an important role. Besides, the local study by Yang (1997) indicates that Formosan Landlocked Salmon is very sensitive to diurnal maximum stream temperature. Thus, the model is designed to consider the effects of mountain shading and to simulate diurnal stream temperature in this study, and then is applied to the ChiChiaWan creek, an important habitat of Formosan Landlocked Salmon.

9.2 MODEL DEVELOPMENT

The proposed stream temperature simulation model takes into account not only solar radiation, longwave radiation, latent heat, sensible heat, but also the effect of shading by surrounding mountains. Thus, a stream network is derived from a DEM first, and then applied to a stream temperature model to evaluate the effect of mountain shading.

Determination of Stream Network

A Digital Elevation Model (DEM) can be applied to determine the stream network. The DEM for Taiwan can be obtained from the Council of Agriculture in Taiwan. There are three major steps to determine the stream network: (1) Adjusting DEM data; (2) Determining flow direction for each grid; (3) Identifying stream network (Pan, 2001).

Adjusting DEM Data

The DEM data may have unreasonable sinks, and often cause problems in determining the stream network. Thus, the first step is to adjust the data. If the height of a grid is lower than the heights of all grids surrounding it, the height of the grid is reassigned as the same as the closest height.

Determining Flow Direction

According to the heights of grids, flow directions for all grids can be determined. By comparing heights of the central grid and surrounding grids, flow direction can be determined and a number is assigned to represent flow directions in computer program. The numbers for eight directions are given as Figure 9.2. Flowing to more than two directions is allowed in this study.

32	64	128
16		1
8	4	2

Figure 9.2 Numbering of flow direction.

Establishment of Stream Network

A unit of uniform overland flow is applied, and then accumulated flow of each grid is estimated to determine the stream network. The flow of a grid runs to the surrounding grid with the lowest height. If there are n grids having the same lowest height, the n grids equally receive 1/n flow. A grid is marked as a stream channel, if its accumulated flow is more than a given threshold.

Stream Temperature Model

Applying the principle of conservation of thermal energy to a one-dimensional vertically well-mixed open channel or stream, the conservative form of the transport equation is shown as equation (1) (Kim and Chapra, 1997).

$$\frac{\partial T}{\partial t}+u\frac{\partial T}{\partial x}=\frac{\partial}{\partial x}(D\frac{\partial T}{\partial x})+\frac{q}{A}(T_L-T)+\frac{H_T w}{c_w\rho_w A}+\frac{H_B p}{c_w\rho_w A} \qquad (1)$$

where T = cross-sectional average stream temperature (^oC); u = mean velocity of stream flow; D = longitudinal dispersion coefficient (m^2/s); T_L = groundwater temperature (^oC); q = groundwater discharge (m^2/s); H_T = surface flux of thermal energy (J/m^2s); w = top width of the channel (m); p = wetted perimeter (m); A = cross sectional area (m^2); H_B = stream bed flux of thermal energy or bed conduction; c_w = specific heat of water (J/kg^oC); ρ_w = density of water (kg/m^3).

Several studies of the dispersion coefficient have been undertaken. A variety of theoretical and empirical relationships have been proposed. In this paper, the dispersion coefficient is computed from equation (2) (Bowie et al., 1985; Brown and Barnwell, 1987; Jobson and Keefer, 1979; Fischer et al., 1979; Kim and Chapra, 1997).

$$D=C_d Ru* \qquad (2)$$

where C_d = dispersion constant, u^* = shear velocity (m/s), and R = hydraulic radius (m).

The dispersion constant generally ranges from about 6 for straight smooth channels to about 500 for some natural channels (Kim and Chapra, 1997). The appropriate value of the dispersion constant can be calibrated by trial and error. The shear velocity is expressed

$$u*=\sqrt{gRS_o} \qquad (3)$$

where g = gravity acceleration (m/s^2) and S_o = slope of river bed. Since the depth of a stream (h) is less than the channel width (w), R can be approximated by h at large width to depth ratios. Substituting (3) into (2) and assuming $R\cong h$ one obtains:

$$D=C_d(gS_0)^{1/2}h^{3/2} \qquad (4)$$

The wetted perimeter (p) can also be approximated using channel width (w) at large width to depth ratios. Equation (1) can now be expressed as

$$\frac{\partial T}{\partial t}+u\frac{\partial T}{\partial x}=\frac{\partial}{\partial x}(D\frac{\partial T}{\partial x})+\frac{q}{A}(T_L-T)+\frac{H_T+H_B}{c_w\rho_w h} \quad (5)$$

The components of thermal affecting the stream include shortwave radiation (R_S), longwave radiation from atmosphere (L_A), stream (L_U), and surroundings (L_T), and latent heat (H_E), sensible heat (H_H), friction heat (H_{fc}), and streambed conduction (H_B). The energy that causes changes of stream temperature is the sum of the thermal fluxes entering stream, and may be expressed as (6).

$$H_T+H_B=(R_s+L_d-L_u+L_T-H_E-H_H+H_{fc})+H_B \quad (6)$$

The second term of right hand side of equation (5) is to consider the thermal brought in by groundwater. In this study, the area-ratio method is used to decide the quantity of groundwater along the simulation reach, which groundwater discharge reaching one point at reach is proportion to its upstream basin area. Then, the mixture of groundwater and the streamflow is considered as in equation (24).

Shortwave Radiation (R_S)

Solar radiation is a major energy source for the ecological systems. The received shortwave radiation was described as

$$R_S=(1-\alpha_P)(1-\alpha_W)\cdot I_0\cdot\sin\beta\cdot(1-M_S) \quad (7)$$

where α_P is planet albedo, α_W is water albedo, I_0 is a solar constant (1362 W/m^2), M_S is an index for mountain shading, and β is the elevation of sun in degrees. The value of β is equal to 90^o - θ_Z, where θ_Z is the zenith angle. The value of α_W depends on β, and can be estimated as in Anderson (1954). The position of the sun, described by the zenith (θ_Z) and azimuth (θ_A) angles, depends on time in a day, date in a year, and latitude. The values of θ_Z and θ_A were determined using the method described by Jansen (1985).

Mountain shading, as shown in Figure 9.3, is considered as a dichotomous variable. Direct shortwave radiation is assumed to be zero when incoming solar radiation is blocked by mountain. In this case, the value of M_s in equation (7) is assigned to be 1. Otherwise M_s=0. The value of M_s depends on the elevation of sun (β) and the maximum angle (θ_S) determined by stream channel and mountain in the direction to sun.

$$M_S=\begin{cases}1 & if\ \theta_S\geq\beta\\ 0 & otherwise\end{cases} \quad (8)$$

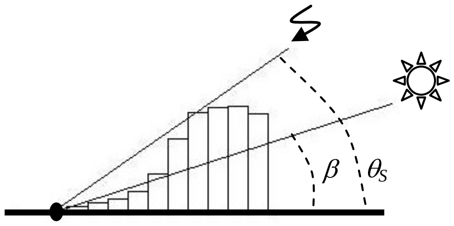

Figure 9.3 Determination of mountain shading.

Longwave Radiation

Longwave radiation includes downward (L_D) and upward radiation (L_U). The upward longwave radiation is emitted by the water body, while downward longwave radiation is emitted by the atmosphere (L_A) and surrounding trees and mountains (L_T).

Radiation emission can be described by Stefan's Law. Water is a gray radiation body and its emitting radiation is given as:

$$L_U = -\varepsilon \cdot \sigma T_W{}^4 \tag{9}$$

where the negative sign on the right hand side of the equation is to represent outgoing energy, ε is effective emissivity and a value of 0.98 (Leblanc et al., 1997) was used in this study, T_W is water temperature (K), and σ is the Stefan-Botzman Constant (5.67×10^{-8} $W/m^2\ K^4$).

The received atmospheric longwave radiation is modified by the sky visible fraction (*SVF*). By considering *SVF*, L_A can be determined as equation (10):

$$L_A = SVF \cdot \sigma T_A^4 \tag{10}$$

The value of SVF can be estimated based on the DEM as $SVF = \int_0^{2\pi}\int_0^{\phi} sin\phi\, d\phi\, d\theta$ (Hesieh, 1997; Pan, 2001). Figure 9.4 shows a conceptual diagram to estimate *SVF* for a grid point.

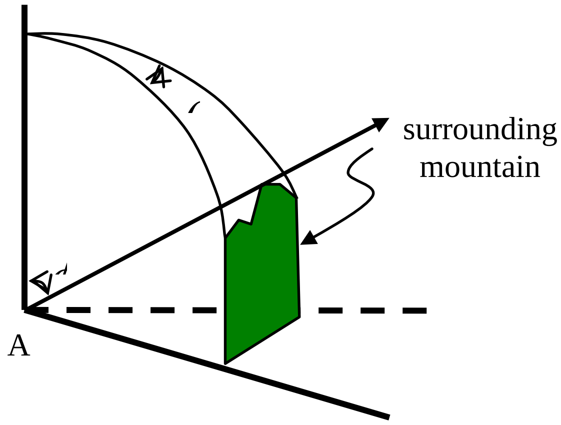

Figure 9.4 A conceptual diagram to estimate SVF.

Surrounding mountains are considered as a grey body; which emit radiation (L_T) calculated as:

$$L_T = SF \cdot \varepsilon\sigma T_A^{\ 4} \tag{11}$$

where SF is a shape factor and can be determined as equation (12). (Lin and Lee, 1989)

$$SF = \int \cos\theta_W \cdot \cos\theta_T \frac{1}{\pi \cdot r^2} dA_T \tag{12}$$

where dA_T is the surrounding area, and θ_W, θ_T, and r are shown in Figure 9.5.

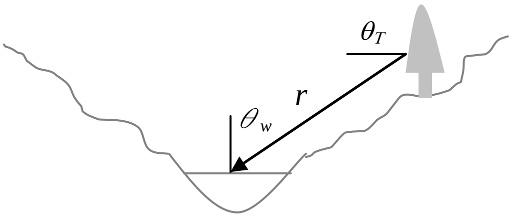

Figure 9.5 The relationships between $\theta_{W,}$ $\theta_{T,}$ and r.

Latent Heat (H_E)

Latent heat is used to vaporize water from the liquid phase to the gas phase, and can be estimated from the equation of evaporation (Edinger et al., 1974).

$$H_E = \left(25.3 + 1.27 \cdot U_W^{\ 2}\right) \cdot \left(e_s - e_a\right) \tag{13}$$

where e_s is saturated vapor pressure, e_a is air vapor pressure, U_W is wind speed.

Sensible Heat (H_H)

Sensible heat can be determined from the latent heat and the Bowen Ratio (B), i.e. $H_H = B \times H_E$. The value of B can be estimated as (Bowen, 1926; Webb and Zhang, 1999)

$$B = 0.61 \cdot \frac{P}{1000} \cdot \left(\frac{T_W - T_A}{e_s - e_a}\right) \tag{14}$$

where P is air pressure (mb), T_W is water temperature (^oC) and T_A is air temperature (^oC).

Friction Heat (H_{fc})

Heat caused by friction between flowing water and streambed can be expressed as (Webb and Zhang, 1999):

$$H_{fc} = 9805 \cdot (F/W) \cdot S_0 \tag{15}$$

where H_{fc} is the friction heat (W/m^2), F is the discharge entering the stream reach (m^3/s), W is the average width of the stream reach (m), and S_0 is the slope of stream reach.

Streambed Conductive Heat (H_B)

This study used the method of computing bed conduction proposed by Jobson (1977). This method considered the streambed as a homogeneous medium insulated on the lower face and with the upper face always having a temperature equal to that of the overlying water. The heat flux into or out of the streambed can then be determined as a function of the past history of the water temperature. Only the thermal diffusivity, heat-storage capacity, and thickness of the medium need to be known. The thickness is arbitrary and can be assumed to be infinity at a considerable cost in computation time.

Carslaw and Jaeger (1959) presented an expression for the temperature distribution within a slab initially at constant temperature for which the upper surface is subjected to a unit increase in temperature at time zero. Analyzing the streambed as a slab insulated on the bottom and of finite thickness L is equivalent to making the assumption that the heat flux through the soil at depths greater than L is insignificant (Jobson, 1977).

$$\Delta T_B(y, i\Delta t) = 1 - \frac{4}{\pi}\sum_{n=0}^{\infty}\frac{(-1)^n}{2n+1}\exp\left[\frac{-\kappa(2n+1)^2\pi^2 \cdot i\Delta t}{4L^2}\right]\cos\left[\frac{(2n+1)\pi y}{2L}\right] \tag{16}$$

where $\Delta T_B(y, i\Delta t)$ = temperature rise within the slab (^{o}C), k = thermal diffusivity (=6.81×10^{-7} m^2/s), L = thickness of the slab (=6m), and y = distance above the insulated bottom of the slab. The increase in the heat content of the slab can be evaluated at any time by multiplying (16) by the heat-storage capacity, then integrating over the total thickness (Jobson, 1977).

$$\phi(i\Delta t) = \rho_S C_S L\left\{1 - \frac{8}{\pi^2}\sum_{n=0}^{\infty}\frac{(-1)^n}{(2n+1)^2}\exp\left[\frac{-\kappa(2n+1)^2\pi^2 \cdot i\Delta t}{4L^2}\right]\sin\left[\frac{(2n+1)\pi}{2}\right]\right\} \tag{17}$$

where $\phi(i\Delta t)$ = increase in heat content of the slab between time 0 and t resulting from the unit increase in surface temperature at time 0; and ρ_s = the density of the slab (steam bed); C_s = the specific heat of the slab. The heat flux to the water, $\Delta\phi(i)$, during any time step $i\Delta t$ to $(i+1)\Delta t$ which results from a unit increase in temperature at time 0, can be computed as (18)

$$\Delta\phi(i) = \phi(i\Delta t) - \phi[(i+1)\Delta t] \tag{18}$$

The $\Delta\phi(i)$ values describe the time variation of the response of the system to a unit change in water temperature.

Equation (18) is linear with respect to temperature, and since water temperature fluctuation can be represented by a series of step changes, the convolution principle is used to determine the heat flux from the bed to the water for any temperature history by use of (19).

$$H_B\left(i\Delta t\right) = \sum_{j=s}^{i} \Delta T_W\left(j\Delta t\right)\cdot \Delta\phi\left(i-j\right) \tag{19}$$

where $H_B(i\Delta t)$ = heat flux to the water from the bed during time $i\Delta t$ to $(i+1)\Delta t$, $\Delta T_W(j\Delta t)$ = changes in water temperature that occurred at $j\Delta t$ ($j \le i$), $\Delta\phi$ is given by (18), and the water temperature is assumed to have been constant for time before t=-$s\Delta t$. Equation (19) can be solved for each grid point and each time step in a temperature model (Jobson, 1977).

Numerical Method

The Crank-Nicholson method (Yogeh and Kenneth, 1986) is used to solve equation (5). The partial derivative in time and the first and second derivative in space can be shown below.

$$\frac{\partial f}{\partial t} \approx \frac{f_j^{n+1} - f_j^n}{\Delta t} \tag{20}$$

$$\frac{\partial f}{\partial x} \approx \frac{1}{2}\left(\frac{f_{j+1}^{n+1} - f_{j-1}^{n+1}}{2\Delta x} + \frac{f_{j+1}^{n} - f_{j-1}^{n}}{2\Delta x}\right) \tag{21}$$

$$\frac{\partial^2 f}{\partial x^2} \approx \frac{1}{2}\left[\frac{f_{j+1}^{n+1} - 2f_j^{n+1} + f_{j-1}^{n+1}}{(\Delta x)^2} + \frac{f_{j+1}^{n} - 2f_j^{n} + f_{j-1}^{n}}{(\Delta x)^2}\right] \tag{22}$$

$$f \approx \frac{1}{2}\left(f_j^{n+1} + f_j^n\right) \tag{23}$$

where n is the number of time period and j is a spatial grid number. Substituting equation (20) to (23) into equation (5), the following expression for a segment from x_{j-1} to x_{j+1} is obtained.

$$\begin{aligned}
&\left(-\frac{1}{2}u_j^{n+1} - \frac{D_{j-1/2}^{n+1}}{\Delta x}\right)T_{j-1}^{n+1} + \left(2\frac{\Delta x}{\Delta t} + \frac{D_{j+1/2}^{n+1} + D_{j-1/2}^{n+1}}{\Delta x} + \Delta x\frac{q_j^{n+1}}{A_j^{n+1}}\right)T_j^{n+1} + \left(\frac{1}{2}u_j^{n+1} - \frac{D_{j+1/2}^{n+1}}{\Delta x}\right)T_{j+1}^{n+1} \\
&= \left(\frac{1}{2}u_j^{n} - \frac{D_{j-1/2}^{n}}{\Delta x}\right)T_{j-1}^{n} + \left(2\frac{\Delta x}{\Delta t} - \frac{D_{j+1/2}^{n} + D_{j-1/2}^{n}}{\Delta x} - \Delta x\frac{q_j^{n}}{A_j^{n}}\right)T_j^{n} + \left(-\frac{1}{2}u_j^{n} + \frac{D_{j+1/2}^{n}}{\Delta x}\right)T_{j+1}^{n} \\
&+ \Delta x\left[\frac{q_j^n}{A_j^n}(T_L)_j^n + \frac{q_j^{n+1}}{A_j^{n+1}}(T_L)_j^{n+1}\right] + \frac{\Delta x}{C_w\rho_w}\left[\frac{(H_T + H_B)_j^n}{h_j^n} + \frac{(H_T + H_B)_j^{n+1}}{h_j^{n+1}}\right]
\end{aligned} \tag{24}$$

Equation (24) for all grids can be written in the matrix form as equation (25).

$$\boldsymbol{C} \bullet \boldsymbol{T} = \boldsymbol{K} \tag{25}$$

where matrix ***C*** represents the coefficients of the left hand side of equation (24), and matrix ***K*** represents the constants of the right hand side of equation (24). Matrix ***T*** stands for unknown water temperatures in the next time step. Because emission radiation from river, $(L_u)_j^{n+1}$ is a function of T_j^{n+1} and unknown, an iterative method is used to solve water temperatures of all grids in the next time step. Besides, matrix ***C*** is a tridiagonal matrix. Thomas algorithm which provides more calculating efficiency and less error (Yogeh and Kenneth, 1986) and is used to solve equation (25). Moreover, two sets of boundary conditions and one set of initial condition are also needed.

9.3 Study Site

Site Description

The ChiChiaWan Creek is a major Formosan Landlocked Salmon habitat and thus was selected as a study site in this investigation. The watershed is located between 24°20’ and 24°25’ north and between 121°10’ and 121°20’ east, and the river length and catchment area are 15.3 km and 56 km^2, respectively. The average annual streamflow is 5.4 m^3/s measured at the ChiChiaWan gauge station. Streamflow is significantly different in wet (May through October) and dry seasons (November through April), with 70% of annual stream flow occurring during the wet season. The land uses of the ChiChiaWan watershed include natural forest, reforested areas, meadow, fallow areas, tea croplands, and orchards. Forest occupies 88.4% of the watershed. Meadow and fallow areas cover 10%, while orchards and tea gardens encompass 1.5% of land use (Tung and Lee, 2001). The average elevation is about 1700m and the average slope is about 25 to 30%. Because the cliffs are very close to the river in the ChiChiaWan Creek, the shading effect of terrain is very important when compute the solar radiation

This study focuses on assessing the impact of climate change on stream temperature of Formosan Landlocked Salmon habitats. The reach between Dam1 and Dam3 in the ChiChiaWan Creek (Figure 9.1) is one of the main habitats of Formosan Landlocked Salmon and is selected as a study case. The distances between Dam1 and Dam3 are 4349 *m*. The stream temperature in this reach is simulated and compared with observations at Dam2 to verify the stream temperature model.

Data

The inputs of the stream temperature model include meteorological data and hydrological data, which were recorded in the SungMao and HuanShan weather station and ChiChiaWan streamflow gauge station, respectively.

Meteorological Data

The meteorological data, including air temperature, relative humidity, atmospheric pressure and wind speed, are used to calculate the energy balance. Three days with clear sky, 1997/8/3, 1997/8/4, 1996/10/6, are chosen. The meteorological data of chosen dates are shown in Table 9.1.

Table 9.1 Weather data for model calibration and validation.

	Calibration	Validation	
Date	1997/8/3	1997/8/4	1996/10/6
Maximum air temperature (^oC)	27.0	27.0	25.2
Minimum air temperature (^oC)	15.8	15.1	10
Relative humidity (%)	81	78	77
Atmospheric pressure (mb)	639	640	642
Wind speed（m/s）	0.7	1.6	0.9
Stream flow (cms)	2.65	2.53	3.55

Hydrological Data

Hydrological data include stream width, depth and flow velocity. There have been many researches showing the functional relations between stream width (w), depth (h) and stream flow (Q) shown as equation (26) and (27). The parameters are determined by regression analysis with observed data and listed in the Table 9.2.

$$w = aQ^b \tag{26}$$

$$h = cQ^d \tag{27}$$

Table 9.2 Hydrological parameters for the two reaches

Reach	Parameter			
	a	b	c	d
Dam3 to Dam2	9.3646	0.0125	0.3823	0.2105
Dam2 to Dam1	6.8690	0.2702	0.3613	0.1331

Stream average velocity (u) within a grid is calculated by $u = \frac{Q}{w \cdot h}$. The discharge flowing through a grid is estimated as recorded streamflow multiplied by an area ratio which is the subcatchment area of the grid to the area of the gauge station. The subcatchment area for each grid can be estimated based on the DEM.

Since groundwater temperature is 1~2 ^oC higher than annual average air temperature (Collins, 1925; Heath, 1964; Todd, 1980), groundwater temperature is assumed to be annual average air temperature plus 1^{o}C. The annual average air temperature in the study site is 15^{o}C, and thus the groundwater temperature is set to be 16 ^{o}C for current climate condition.

9.4 Climate Change Impacts Assessment

A procedure to assess the climate change impact is described in this section. First, future climate change scenarios are derived from GCM predictions, and a weather generation model (Pickering et al., 1988) is applied to produce daily weather data based on climate scenarios. Secondly, generated daily air temperature and simulated streamflow in different climate conditions must be done before evaluating the climate change impacts.

Climate Change Scenarios

Climate scenarios are derived from different GCMs and different experiments, including equilibrium experiments and transition experiments based on SRES (Special Report on Emissions Scenarios), respectively. The change of future temperature in the study area is assumed to be the same as the difference between the temperatures simulated by GCMs for future and current conditions in the nearest grid point. Thus, future climate scenarios can be estimated as

$$\mu'_{mT} = \mu_{mT} + (\mu_{mT,Future} - \mu_{mT,Current}) \quad (28)$$

where μ_{mT} and μ'_{mT} are current and future mean monthly temperature (^{o}C), respectively, $\mu_{mT,current}$ and $\mu_{mT,Future}$ are simulated mean monthly temperatures (^{o}C) under current and future climate conditions, respectively. The change in precipitation is assumed to be the ratio of the precipitation for future conditions to that for current conditions:

$$\mu'_{mP} = \mu_{mP} \times (\mu_{mP,Future} / \mu_{mP,Current}) \quad (29)$$

where μ_{mP} and μ'_{mP} are current and future mean monthly precipitation (cm), respectively, $\mu_{mP,Current}$ and $\mu_{mP,Fuuture}$ are simulated mean monthly precipitation (cm) under current and future climate conditions, respectively.

The predictions of the GCM equilibrium experiments (1995 version) are downloaded from US Country Studies Program in the NCAR ftp site (ftp://ncardata.ucar.edu/pub). Outputs from two models are used, namely the CCCM (Canadian Centre for Climate Modelling and Analysis) and GISS (Goddard Institute for Space Studies) models. The change of mean monthly temperature and the ratio of precipitation between $1\times$CO2 and $2\times$CO2 conditions are listed in Table 9.3.

The climate simulations of the transition experiment by CGCM2 (Canadian Centre for Climate Modelling and Analysis) and HADCM3 (Hadley Centre for Climate Prediction and Research) based on A2 scenario of SRES are also used to setup other future climate scenarios. Three future periods are considered, including the short-term (2010~2039), mid-term (2040~2069), and long-term (2070~2099) scenarios. The future climate scenarios are also determined by equations (28) and (29), in which $\mu_{mT,current}$ and $\mu_{mp,current}$ are averaged from GCM predictions for the period of 1961~1990 and the values of $\mu_{mT,Future}$ and $\mu_{mp,Future}$ are average values for the appropriate future periods. The GCM output data can be obtained from the IPCC Data Distribution Centre (http://ipcc-ddc.cru.uea.ac.uk/dkrz/dkrz_index.html). The climate changes estimated based on the A2 scenario for the study site are given in Table 9.4.

Table 9.3 Changes of mean monthly temperature (ΔT, ^oC) and ratios of mean monthly precipitation (*Rp*, *cm/cm*) – equilibrium experiments.

Month	CCCM		GISS	
	ΔT	R_p	ΔT	R_p
1	2.71	0.81	2.74	1.13
2	3.66	1.05	2.59	0.68
3	4.73	0.67	3.31	1.03
4	4.16	1.11	3.75	1.33
5	4.21	1.13	3.58	0.91
6	2.52	1.39	4.69	1.51
7	2.09	1.00	4.52	1.30
8	1.75	1.19	4.18	1.23
9	2.62	1.40	3.52	1.30
10	2.45	1.01	2.92	0.98
11	2.39	0.86	3.72	1.15
12	3.42	0.66	2.42	0.94
Average	3.02	1.02	3.50	1.12

Table 9.4 Changes of temperature and ratios of precipitation predicted by the CGCM2 and HADCM3 models based on SRES-A2 scenario.

Month	CGCM2						HADCM3					
	ΔT			R_p			ΔT			R_p		
	S	M	L	S	M	L	S	M	L	S	M	L
1	0.94	1.62	2.76	1.22	1.12	1.02	0.84	1.82	3.11	1.13	0.85	0.95
2	1.81	2.57	3.27	1.35	1.01	0.89	0.46	1.55	2.4	0.95	0.68	1
3	1.25	2.64	3.78	1.3	1.03	0.88	0.52	1.44	2.45	0.95	1.07	0.92
4	0.6	1.82	4.64	1.13	0.8	0.76	0.61	1.52	2.49	1.13	1.31	1.28
5	-0.46	2.78	4.54	1.1	0.82	0.54	0.29	1.35	2.2	1.08	1.3	1.38
6	1.09	3.62	5.62	1.03	0.79	0.7	0.63	1.35	2.33	1.3	1.21	1.01
7	1.18	2.26	4.52	0.92	0.93	0.7	0.53	1.32	2.28	1.14	1.1	1.37
8	0.52	2.05	3.45	1.19	1.03	1.23	0.4	1.37	2.23	1.21	1.27	1.39
9	0.45	1.9	3.12	1.18	0.97	1.29	0.6	1.46	3.04	1.27	0.98	1.25
10	0.43	1.81	2.68	0.92	0.99	1.09	0.91	1.5	2.99	1.07	1.53	1.47
11	0.47	2.1	2.53	1.1	1.24	0.8	0.75	1.47	2.59	0.85	0.8	0.91
12	1.41	2.43	2.81	0.96	0.88	0.69	0.9	1.75	3.1	1.08	1	0.88
average	0.81	2.30	3.64	1.12	0.97	0.88	0.62	1.49	2.60	1.10	1.09	1.15

S : Short-term 2010~2039; M : Mid-term 2040~2069; L : Long-term 2070~2099

Impact Assessment

The stream temperature for different climate scenarios is estimated based on the related meteorological and hydrological data. Thus, all the input data under different climate scenarios need to be evaluated first. In addition, the climate change impacts on upper boundary stream temperature and groundwater need also to be determined.

Daily weather data are required for the stream temperature model and to simulate future streamflows. Thus, the weather generation model (Pickering, et al. 1988; Tung and Haith, 1995) is applied to generate daily air temperature and precipitation for different climate scenarios. A sequence of 100-years of daily precipitation and air temperature is generated for each current or future climate scenario.

The daily stream temperature is simulated based on shortwave radiation on 15th day of each month, average air temperature, and average streamflow. The monthly average streamflows are obtained from averaging streamflows simulated by the streamflow component of the Generalized Watershed Loading Functions (GWLF) (Haith and Shoemaker, 1987; Haith et al., 1992) (Lee, 2003). The streamflow model is a conceptual water balance model and has been verified to provide reasonable streamflow predictions for the ChiChaWan creek by Tung and Lee (2001). The streamflow model needs daily temperature and precipitation as inputs.

The upper boundary condition in the stream temperature model under different climate scenarios are estimated according to the monthly changes of air temperature. Stefan and Preud'homme (1993) suggested that the increase of 1 ^{o}C in air temperature may cause increase of 0.75 ^{o}C in stream temperature. The observed stream temperatures of Dam3 on 15th day of each month in 1998 are taken as current stream temperature. The future upper boundary stream temperatures are assumed to be current stream temperature plus the change of air temperature multiplied by 0.75.

There is no further information for groundwater from the study site, which limits further study on the climate change impacts on groundwater temperature. Because groundwater temperature is 1~2 ^{o}C higher than annual average air temperature (Collins, 1925; Heath, 1964; Todd, 1980), 1 ^{o}C is added to annual average air temperatures of different climate conditions to represent their groundwater temperatures.

9.5 Results and Discussions

The verification results of the proposed model are addressed first. Then, the climate change impacts of different climate scenarios are given.

Verification

The procedure to determine the stream network is applied to the ChiChiaWan creek based on DEM with a resolution of 40m×40m. Comparing with map and other digitized stream network by other independent studies, the determined major stream networks are alike. However, quantification analysis is not done, which may bring uncertainty for stream temperature simulation.

Most of parameters in the proposed stream temperature model can be estimated based on watershed and river channel characteristics directly. Only dispersion constant (C_d) and thickness of the slab (L) in equation (17) are required further calibrated by trial and error. The input data and observed stream temperature on 1997/8/3 are used to calibrate the parameters for the stream temperature model. The results indicate that the model is not sensitive to the two parameters in the study reach. The calibrated and observed stream temperature is shown in Figure 6. The values of 500m^2/s for C_d as suggested by Kim and Chapra (1997) and 6 m for L as used in Jobson (1977) are further applied to validate the model for 1997/8/4 and 1996/10/6, and results are shown in Figures 7 and 8, respectively. The results of calibration and validation are summarized in Table 9.5. According to the results, the stream temperature model developed in this study could reasonably simulate diurnal stream temperature. The root mean square errors (RMSE) are all below 1 ^{o}C, and the differences between observed and simulated maximum stream temperature are below 0.4 ^{o}C. The larger RSME is due to the time lag between observed and simulated stream temperatures. The time lag may be caused by the simplification of hydrological data, such as the assumption of rectangular channel and continuity equation while estimating stream velocity. However, the simulated results are reasonable, especially the daily maximum stream temperature, and thus the stream temperature model is further applied to assess the impacts of climate change.

Table 9.5 The results of calibration and validation studies.

			Dam2	Dam1
Calibration	1997/8/3	$T_{max,obs}$	17.02	17.88
		$T_{max,sim}$	16.99	18.25
		ΔT_{max}	0.03	0.37
		RMSE	0.74	0.92
Validation	1997/8/4	$T_{max,obs}$	17.49	18.85
		$T_{max,sim}$	17.32	18.52
		ΔT_{max}	0.17	0.33
		RMSE	0.76	0.80
	1996/10/6	$T_{max,obs}$	14.64	16.12
		$T_{max,sim}$	14.80	16.14
		ΔT_{max}	0.16	0.02
		RMSE	0.41	0.54

$T_{max,obs}$ and $T_{max,sim}$: Observed and simulated maximum stream temperature
ΔT_{max} : Difference between $T_{max,obs}$ and $T_{max,sim}$
RMSE : Root mean square error of diurnal stream temperature

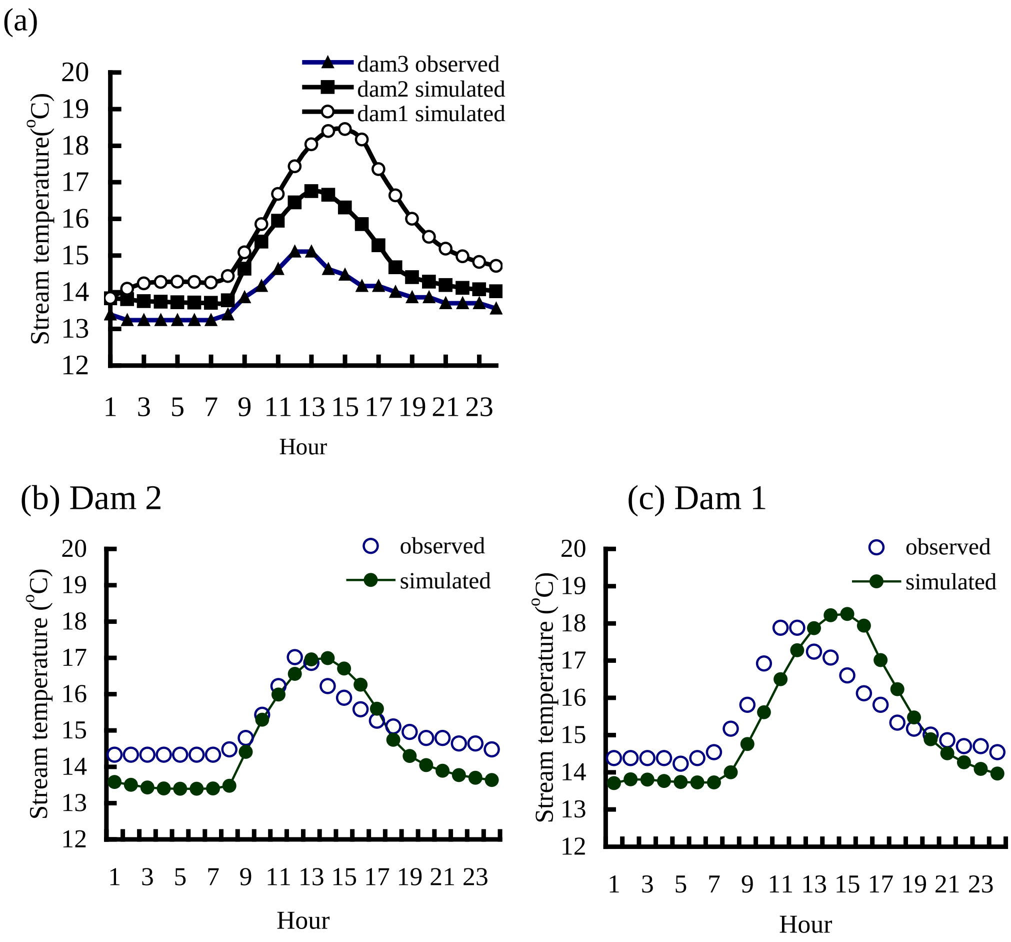

Figure 9.6 (a) Simulated water temperature at Dam 2 and Dam 1 using observed water temperature at Dam 3 as boundary condition. The observed and simulated stream temperature on 1997/8/3 at (b) Dam2; (c) Dam1; – calibration study.

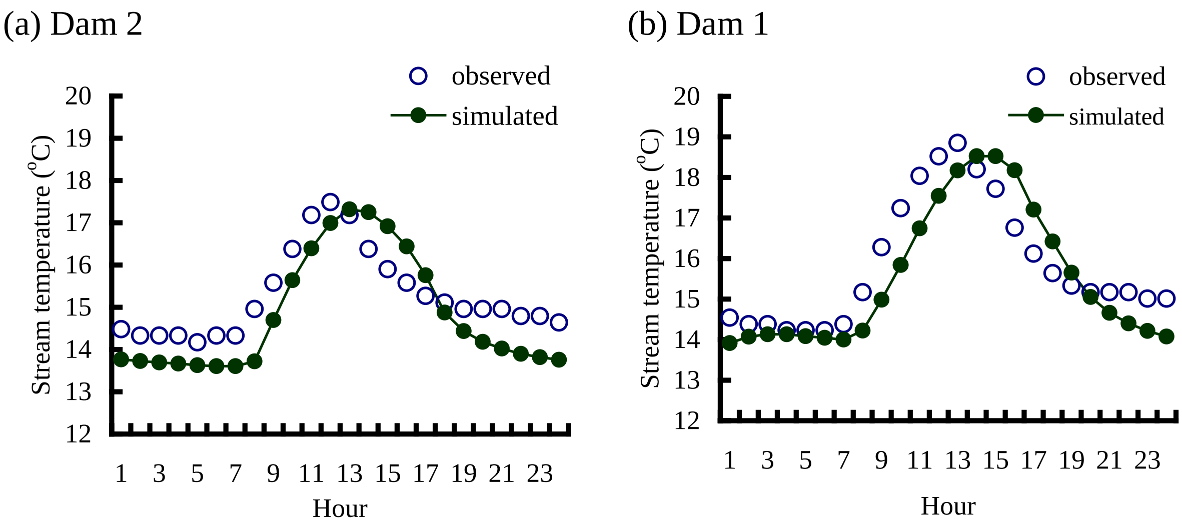

Figure 9.7 The observed and simulated stream temperature on 1997/8/4 at (a) Dam2; (b) Dam1 – validation study.

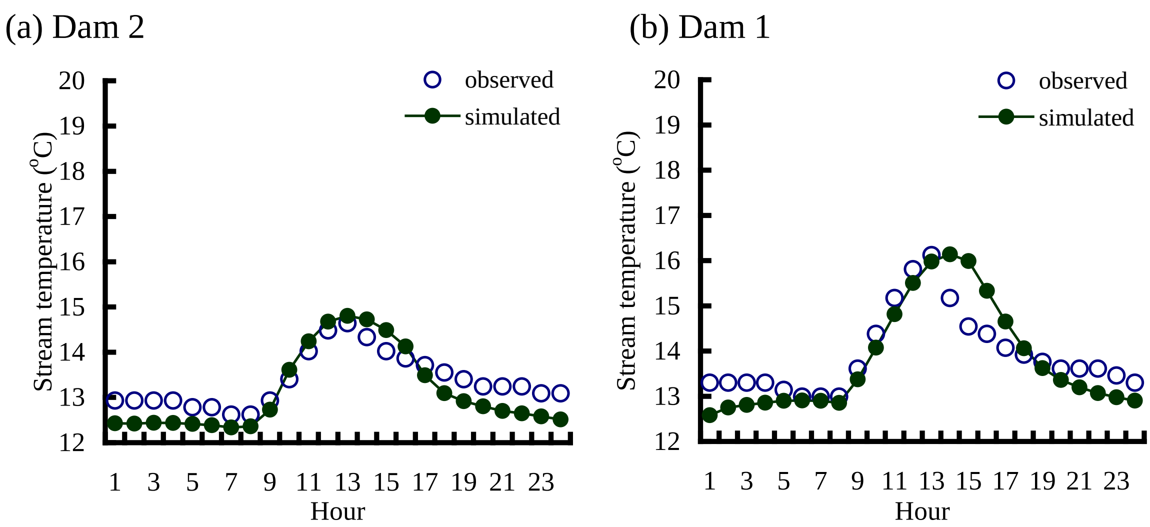

Figure 9.8 The observed and simulated stream temperature on 1996/10/6 at (a) Dam2; (b) Dam1 – validation study.

Climate Change Impacts

The simulated stream temperature for Dam2 is taken as an example. The simulated daily mean and maximum stream temperatures for different climate conditions for each month are summarized in Table 6. An uncertainty analysis is also done to verify whether the changes of daily mean and maximal water temperature are significant at 90% confidence level. The results indicate that most of changes are significant, except of changes of both daily mean and maximum water temperatures in May under CGCM2 short-term scenario and changes of daily maximal temperatures in May, July, and August under HADCM3 short-term scenario.

According to Table 9.6, stream temperatures in some months have exceeded 17 ^{o}C even under current climatic condition and the identical trend of increasing stream temperature can be found for all future climate scenarios. The differences of stream temperature between current and future climate scenarios are shown in Table 9.7 and in Figures 9.9 and 9.10. Annual average stream temperatures are predicted to rise by 0.5 ^{o}C (HADCM3 Short-term) to 2.9 ^{o}C (CGCM2 Long-term), and annual maximum stream temperatures are predicted to rise by 0.5 ^{o}C (HADCM3 Short-term) to 3.2 ^{o}C (CGCM2 Long-term). Moreover, the greatest future increase of stream temperature would occur in summer and will cause most danger to Formosan Landlocked Salmon.

The suitable habitats for Formosan Landlocked Salmon between Dam1 and Dam3 are further surveyed here. A recent research (Tseng, 1999) has shown that suitable stream temperature is between 9~17 ^{o}C and no Formosan Landlocked Salmon can be found in the river when water temperature exceeds over 18 ^{o}C (Lee and Lee, 1996). Thus, two critical stream temperatures of 17 ^{o}C and 18 ^{o}C are applied to determine the stream length of suitable habitats. Figure 9.11 shows the monthly lengths of suitable stream habitats in the current climate condition. The x-axis stands for the downward distance from Dam3, therefore the right side of the x-axis is the location of Dam1. The black and white bars in Figure 9.11 represent the available habitats with the criterion of 18 ^{o}C and 17 ^{o}C, respectively. According to Figure 9.11, it is found that during the periods of January to June and October to December the reaches between Dam3 to Dam1 are suitable habitats with mean stream temperature below 17 ^{o}C in the current climate condition. However, some segments are unavailable for habitats. Taking July as an example, the stream temperature is over 17 ^{o}C for 400m below Dam3 and even more than 18 ^{o}C in downward distance of 3000m from Dam3.

Figures 9.12, 9.13 and 9.14 show the distribution of available stream habitats in the different future climate conditions. In Figures 9.12 and 9.13, the simulations show the sequential impact of climate change according to the magnitude of decreasing available habitats are long-term, mid-term and short-term in whatever future climate conditions. Figure 14 shows the results based on two GCM equilibrium experiments with doubling atmospheric CO_2, and the changes of available habitats are similar to the results of long-term effects. The simulation results show that on average suitable stream habitat would decline by 333m (HADCM3 Short-term) to 1633m (CGCM2 Long-term) using a criterion of 17^{o}C, and by 166m (HADCM3 Short-term) to 1833m (CGCM2 Long-term) using a criterion of 18 ^{o}C, respectively. The most increase of stream temperature and the most loss of available habitat will be in summer in the future climatic conditions.

Table 9.6 Simulated daily mean and maximum stream temperature at Dam2 under different climate conditions.

Scenarios	Daily	Jan	Feb	Mar	Apr	May	Jun	Jul	Aug	Sep	Oct	Nov	Dec
NOW	μ_T	9.1	9.5	11.0	11.5	13.4	13.4	15.3	15.7	14.7	12.7	11.9	10.4
	T_{max}	11.3	11.3	12.6	13.5	15.5	15.4	17.6	17.6	16.9	14.8	14.0	12.7
CGCM2S	μ_T	9.8	10.8	11.9	12.0	13.2*	15.1	16.2	16.1	15.1	13.0	12.3	11.4
	T_{max}	11.9	12.4	13.4	13.9	15.2	17.0	18.5	17.9	17.2	15.2	14.4	13.8
CGCM2M	μ_T	10.4	11.4	13.0	13.0	15.6	17.0	17.2	17.4	16.3	14.1	13.5	12.2
	T_{max}	12.6	13.2	14.7	15.2	17.9	19.2	19.7	19.2	18.5	16.3	15.7	14.6
CGCM2L	μ_T	11.2	12.0	14.0	15.0	17.0	18.6	19.0	18.4	17.3	14.9	13.9	12.3
	T_{max}	13.5	14.0	15.8	17.5	20.1	21.3	22.0	20.3	19.3	17.0	16.2	14.8
HADCM3S	μ_T	9.7	9.8	11.5	11.9	13.7	14.7	15.7	16.0	15.2	13.3	12.4	11.0
	T_{max}	11.8	11.7	13.1	14.0	15.7*	16.6	17.9*	17.8*	17.3	15.4	14.6	13.4
HADCM3M	μ_T	10.4	10.6	12.2	12.6	14.5	15.3	16.4	16.8	15.9	13.8	13.0	11.6
	T_{max}	12.7	12.8	13.9	14.6	16.4	17.2	18.6	18.5	18.0	15.8	15.1	14.0
HADCM3L	μ_T	11.2	11.3	13.0	13.4	15.2	16.1	17.1	17.5	17.1	14.9	13.9	12.6
	T_{max}	13.7	13.3	14.8	15.3	17.0	18.0	19.3	19.2	19.1	16.9	15.9	15.1
CCCM	μ_T	10.9	12.2	14.5	14.6	16.6	16.3	17.1	17.2	16.9	14.7	13.8	12.7
	T_{max}	13.4	14.1	16.5	16.8	18.6	18.1	19.3	19.0	18.9	16.7	16.0	15.2
GISS	μ_T	11.3	11.6	13.6	14.4	16.2	17.7	18.7	18.9	17.5	15.0	14.7	12.3
	T_{max}	13.5	13.6	15.4	16.3	18.3	19.6	20.8	20.6	19.6	17.1	16.9	14.7

μ_T : Daily mean stream temperature

T_{max} : Daily Maximal stream temperature

Table 9.7 The changes of daily mean and maximum stream temperature (°C) at Dam2.

Scenarios	Month	Jan	Feb	Mar	Apr	May	Jun	Jul	Aug	Sep	Oct	Nov	Dec
CGCM2S	$\Delta\mu_T$	0.8	1.3	0.9	0.5	-0.2*	1.6	0.9	0.4	0.4	0.4	0.4	1.0
	ΔT_{max}	0.7	1.1	0.7	0.4	-0.3*	1.6	0.9	0.4	0.3	0.4	0.4	1.0
CGCM2M	$\Delta\mu_T$	1.3	2.0	2.0	1.5	2.2	3.5	1.8	1.6	1.5	1.5	1.7	1.8
	ΔT_{max}	1.3	2.0	2.0	1.7	2.4	3.8	2.1	1.7	1.6	1.5	1.6	1.9
CGCM2L	$\Delta\mu_T$	2.1	2.6	2.9	3.5	3.6	5.1	3.6	2.7	2.5	2.2	2.1	1.9
	ΔT_{max}	2.3	2.7	3.1	4.0	4.6	5.9	4.4	2.7	2.4	2.2	2.1	2.0
HADCM3S	$\Delta\mu_T$	0.7	0.4	0.4	0.5	0.3	1.3	0.4	0.3	0.5	0.7	0.6	0.6
	ΔT_{max}	0.6	0.4	0.5	0.4	0.2*	1.2	0.3*	0.2*	0.4	0.6	0.6	0.7
HADCM3M	$\Delta\mu_T$	1.3	1.2	1.1	1.2	1.0	1.9	1.0	1.1	1.1	1.2	1.2	1.2
	ΔT_{max}	1.4	1.5	1.2	1.0	0.9	1.8	1.0	1.0	1.1	1.0	1.1	1.3
HADCM3L	$\Delta\mu_T$	2.2	1.9	1.9	2.0	1.7	2.7	1.8	1.8	2.3	2.3	2.0	2.2
	ΔT_{max}	2.4	2.1	2.1	1.8	1.5	2.6	1.7	1.6	2.2	2.1	1.9	2.3
CCCM	$\Delta\mu_T$	1.9	2.8	3.5	3.1	3.1	2.8	1.7	1.5	2.1	2.0	1.9	2.3
	ΔT_{max}	2.2	2.9	3.9	3.3	3.1	2.7	1.7	1.5	2.0	1.9	2.0	2.4
GISS	$\Delta\mu_T$	2.2	2.1	2.6	2.9	2.8	4.3	3.4	3.2	2.8	2.4	2.9	1.9
	ΔT_{max}	2.2	2.4	2.7	2.8	2.9	4.2	3.2	3.1	2.7	2.3	2.9	1.9

* : Insignificant change at 90 significant level

9.6 Conclusions

A stream temperature model is developed to simulate stream temperature and applied to assess the impacts of climate change on stream temperature and available habitats of the ChiChiaWan Creek. This model is designed to include the effect of surrounding topography based on a DEM. The results indicate annual average and maximum stream temperatures are predicted to rise by 0.5~2.9 °C and 0.5~3.2 °C, respectively. In addition, monthly average available habitats would decline by 333m~1633m with the 17°C criterion and 166m~1833m with the 18 °C criterion, respectively. Similar trends of increasing stream temperature and decreasing available habitats are noticed for all climate change scenarios. Since the impacts are caused by global changes, not only local conservation measures but also mitigation strategies for climate change impacts are necessary. The most important mitigation strategy for Formosan Landlocked Salmon might include finding new habitats which are the least sensitive to climate change. The stream temperature model developed in this study will be further applied to different creeks in Taiwan to assess the sensitivity of stream temperature to provide suggestions for Formosan Landlocked Salmon conservation.

Some thermal components or parameters, such as streambed heat flux and dispersion constant, in the proposed model may play insignificant role for some study areas. A sensitivity analysis is suggested, which can simplify estimation of model parameters. Further studies are also proposed to improve the accuracy of the stream temperature model. First, the effects of dams and the morphology of river can be modeled in greater detail future studies, including the use of field information on parameters, such as river depth, flow velocity, etc..

Second, climate change may influence shallow groundwater temperature and cause further impacts on surface water temperature. Since groundwater is the major water source to stream channel during dry periods, which often have the most critical stream temperatures, it will be important to improve the accuracy of estimating the climate change impacts on groundwater temperature. Third, the uncertainty in the setting of upper boundary conditions of stream temperature in solving equation (25) for future climate conditions requires further study.

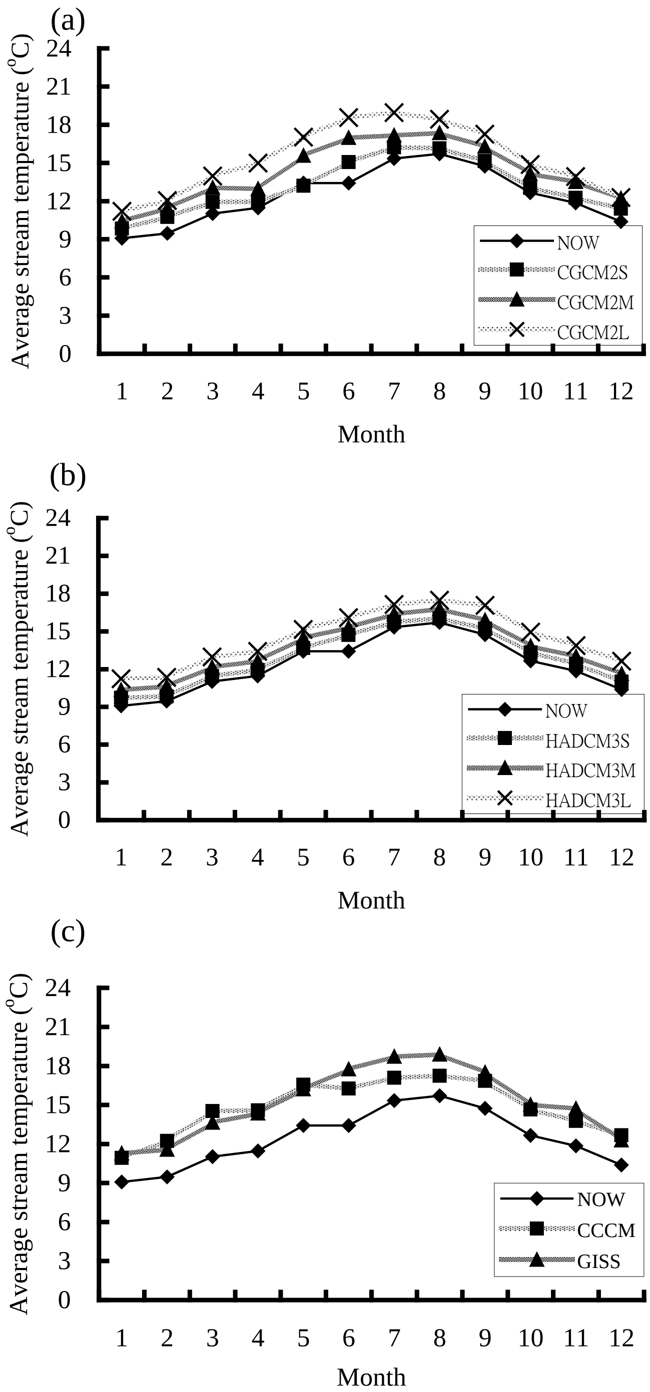

Figure 9.9 Simulated future average stream temperature (a) CGCM2S, CGCM2M, CGCM2L; (b) HADCM3S, HADCM3M, HADCM3L; (c) CCCM and GISS scenarios.

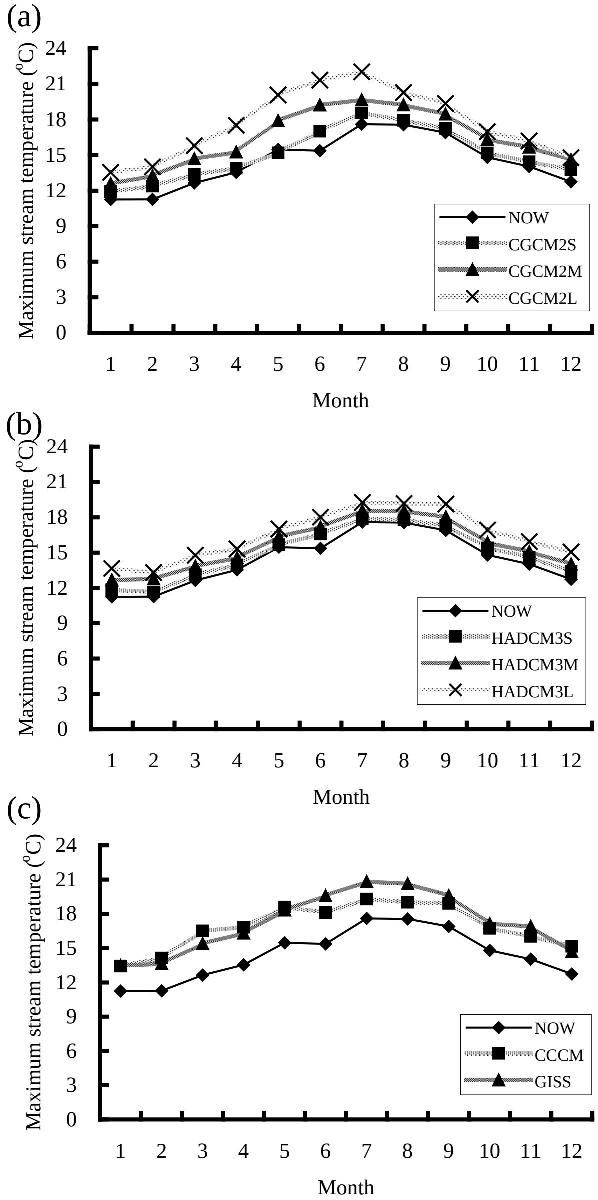

Figure 9.10 Maximum stream temperature under (a) CGCM2S, CGCM2M, CGCM2L; (b) HADCM3S, HADCM3M, HADCM3L; (c) CCCM and GISS scenarios.

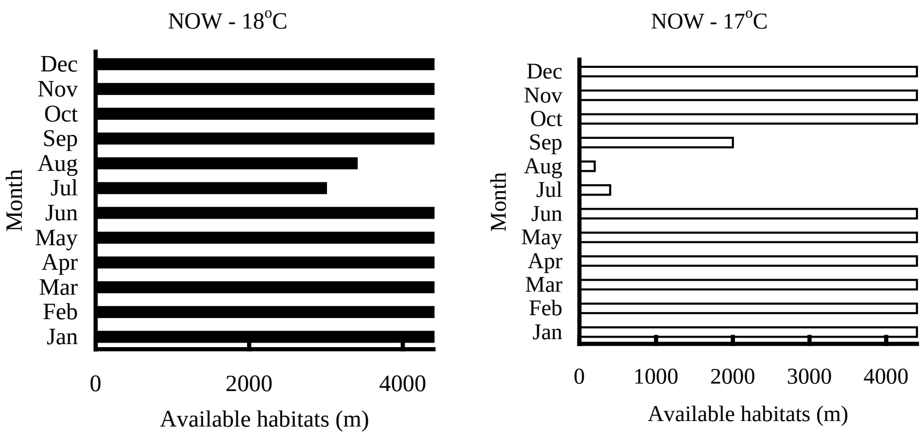

Figure 9.11 Monthly available stream habitats under current climate condition.

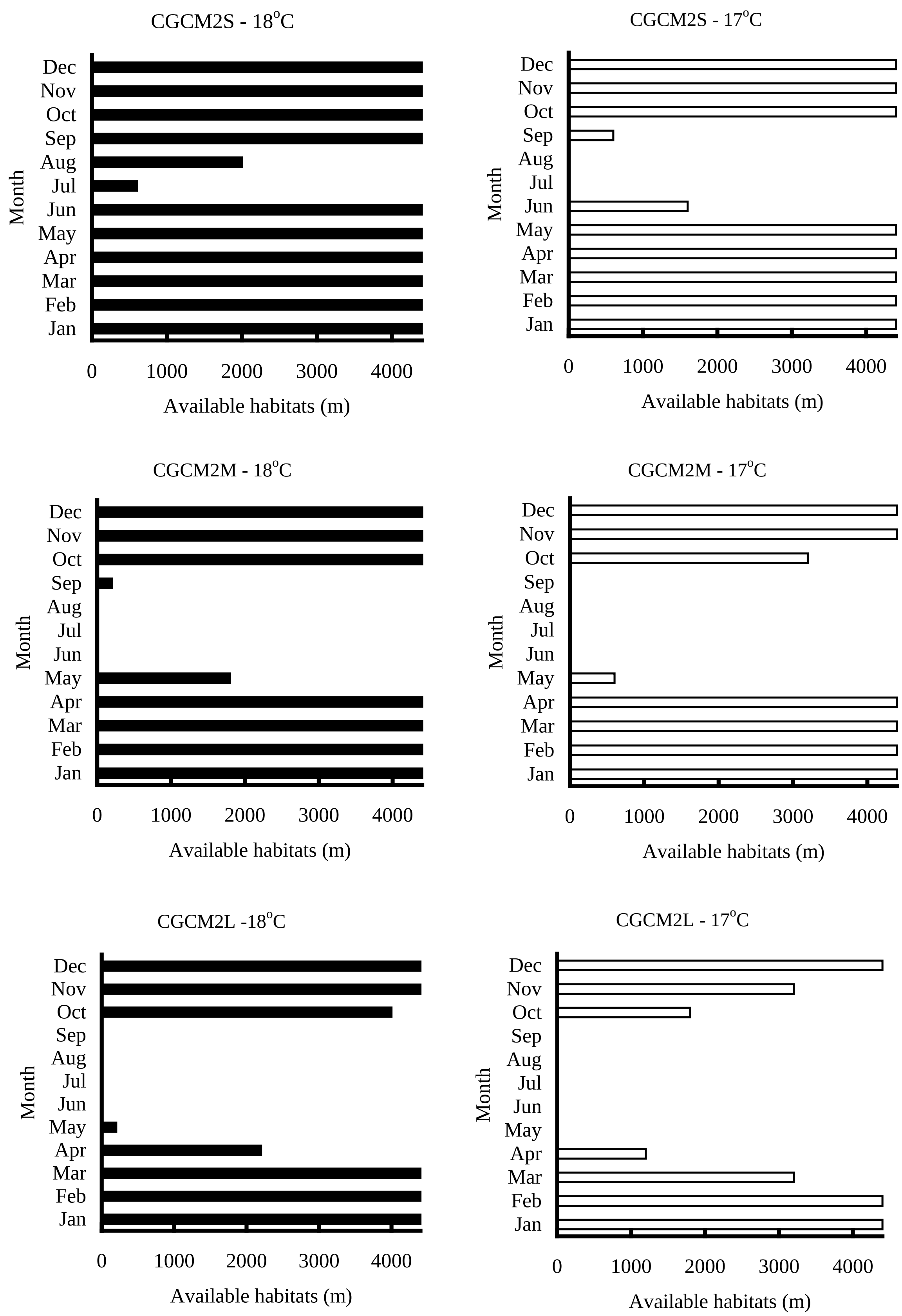

Figure 9.12 Monthly available stream habitats under (a) CGCM2S; (b) CGCM2M; (c) CGCM2L scenarios.

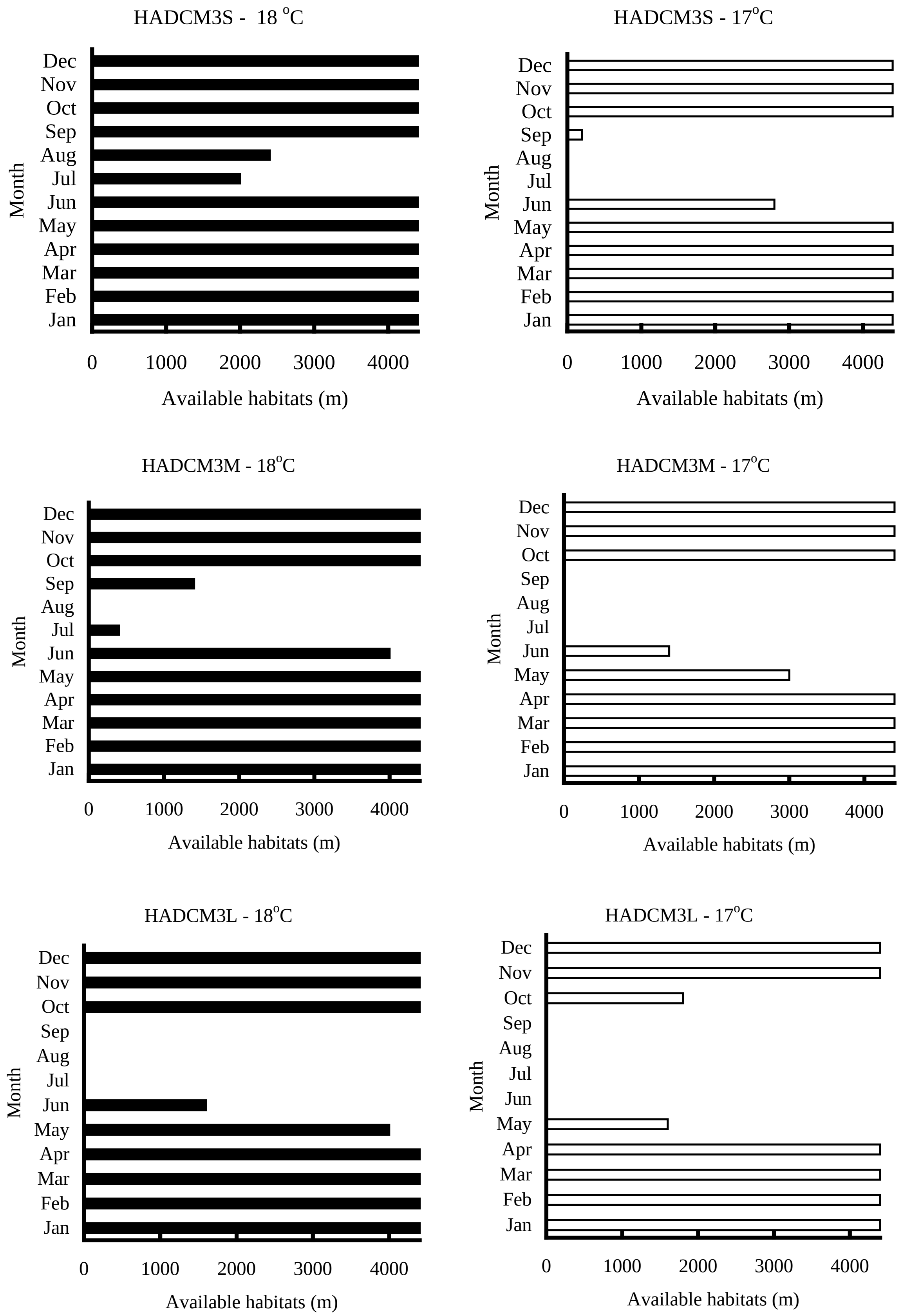

Figure 9.13 Monthly available stream habitats under (a) HADCM3S; (b) HADCM3M; (c) HADCM3L scenarios.

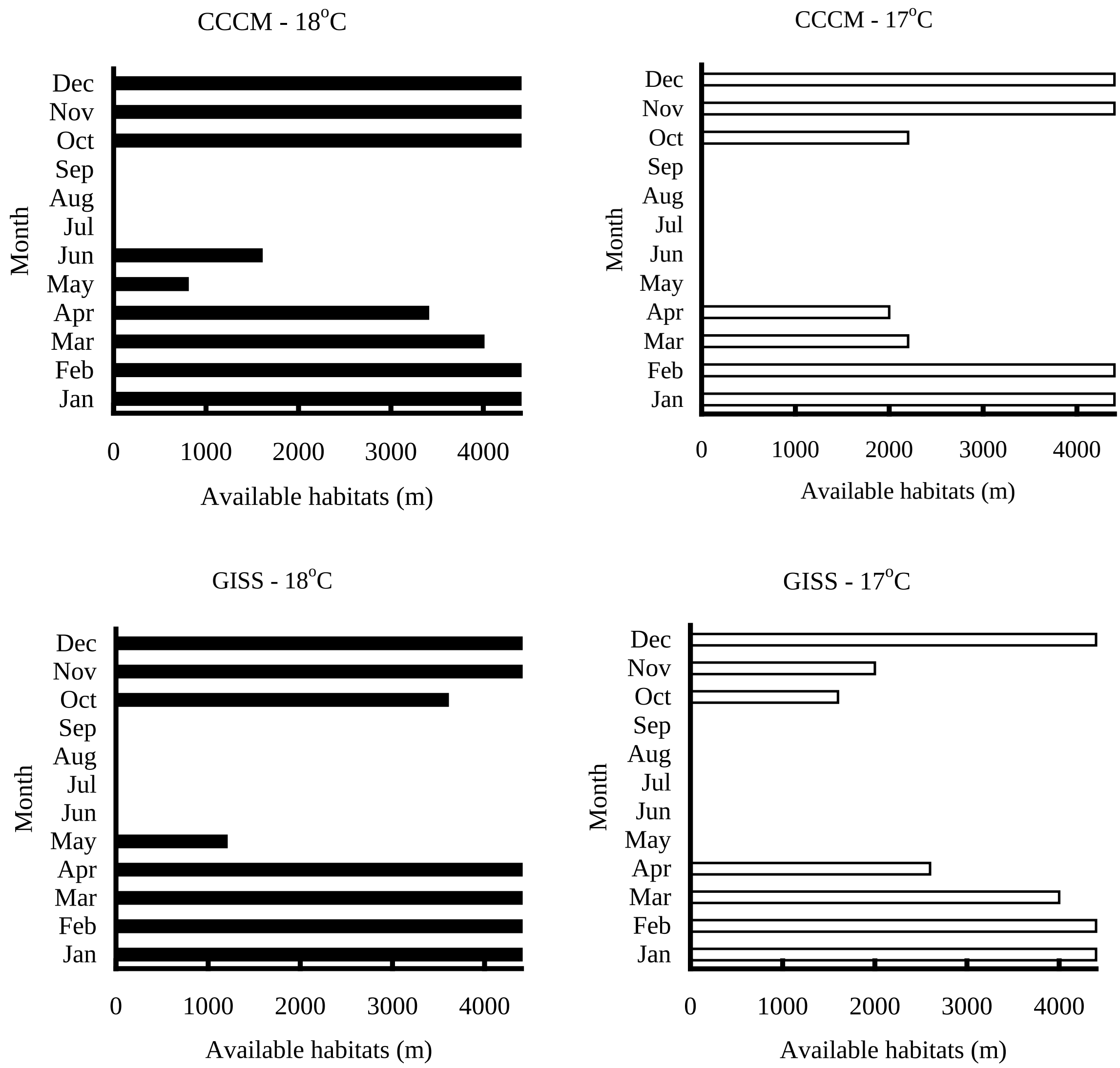

Figure 9.14 Monthly available stream habitats under (a) CCCM; (b) GISS scenarios.

REFERENCES

Anderson ER. 1954. Water loss investigation: Lake Hefner studies. U. S. Department of the Interior. Geology.

Bowen IS. 1926. The ratio of heat losses by conduction and by evaporation from any water surface. *Physical Review* **27**: 779-787.

Bowie GL et al. 1985. Rates, constants, and kinetics of formulation in surface water quality modeling. 2nd Ed. Rep. EPA 600/3-85/040. U.S. Environmental Protection Agency. Athens.

Brown LC and Barnwell Jr, TO. 1987. The enhanced stream water quality models QUAL2E and QUAL2E-UNCAS: documentation and user model. Rep. EPA/600/3-87/007. U.S. Environmental Protection Agency.

Brown GW. 1969. Predicting temperatures of small streams. *Water Resources Research* **5**(1): 68-75.

Brown GW. 1970a. Predicting the effect of clear cutting on stream temperature. *Journal of Soil and Water Conservation* **25**(1): 11-13.

Brown GW. 1970b. Effects of clear-cutting on stream temperature. *Water Resources Research* **6**(4): 1133-1139.

Carslaw HS and Jaeger JC. 1959. *Conduction of Heat in Solids*. 2nd ed. Oxford University Press: New York; 104.

Collins WD. 1925. Temperature of water available for industrial use in the United States. *United States Geological Survey Water Supply Paper* 520-F.

Edinger JE, Brady DK and Geyer JC. 1974. Heat exchange and transport in the environment. *Rep. No. EA-74-049-00-3. Electric Power Res. Inst. Publ*. Palo Alto. California.

Fischer HB, List EJ, Koh RCY, Imberger J and Brooks NH. 1979. *Mixing in land and coastal waters. Academic Press*: New York.

Heath RC. 1964. Seasonal temperature fluctuations in surficial sand near Albany. *United States Geological Survey Professional Paper* 475-D. New York.

Hesieh HC. 1997. Applying a digital terrain model to derive forest habitat factors- a geographic information system approach. *Taiwan Journal of Forest Science* **12**(1): 1-14.

IPCC Working Group Ⅰ. 2001. *Climate change, 2001-The Scientific Basis: Contribution of Working Group Ⅰ, to the third Assessment Report of the Intergover nmental Panel on Climate Change*. Edited by J. T. Houghton, Y. Ding, D. J. Griggs, M. Noguer, P. J. van der Linden, X. Dai, K. Maskell, C. A. Johnson. Cambridge University Press: Cambridge; 881.

Jansen TJ. 1985. *Solar Engineering Technology*. Prentice-Hall Inc. Englewood Cliffs: New Jersey.

Jobson HE. 1977. Bed conduction computation for thermal models. *Journal of Hydraulics Division* **103**(HY10): 1213-1217.

Jobson HE and Keefer TN. 1979. Modeling highly transient flow, mass, and heat transport in the Chattahoochee River near Atlanta. *Georgia. Profl. Paper* 1136. U.S. Geological Survey. Washington D.C.

Kim KS and Chapra, SC. 1997. Temperature model for highly transient shallow streams. *Journal of Hydraulics Engineering* **123**(1): 30-40.

Leblanc RT, Brown RD and FitzGibbon JE. 1997. Modeling the effects of land use change on the water temperature in unregulated urban streams. *Journal of Environmental Management* **49**: 445-469.

Lee PF and Lee YC. 1996. *Monitoring the ChiChiaWan Creek Watershed by Remote Sensing*. The Department of Domestic Affairs. The Bureau of Construction, ShueBa National Park Management Office: Taiwan.

Lee TY. 2003. *The Impacts of Climate Change on Stream Temperature of Formosan Landlocked Salmon's Habitat and Its Population*. The Graduated Thesis of Graduate Institute of Bioenvironmental Systems Engineering. National Taiwan University, Taiwan.

Lin KT and Lee SR. 1989. *Heat Transfer*, New Technology: Taiwan.

Mohseni O, Erickson TR and Stefan HG. 1999. Sensitivity of stream temperatures in the United States to air temperatures projected under a global warming scenario. *Water Resources Research* **35**(12): 3723-3733.

Pan HH. 2001. *The Impacts of Environmental Changes on Stream Temperature of Formosan Landlocked Salmon's Habitat*. The Graduated Thesis of Graduate Institute of Bioenvironmental Systems Engineering. NTU: Taiwan.

Pickering NB, Stedinger JR, and Haith DA. 1988. Weather input for nonpoint models. *Journal of Irrigation and Drainage*. 114(4): 674-690.

Stefan HG and Preud'homme EB. 1993. Stream temperature estimation from air temperature. *Water Resources Bulletin* **29**(1): 27-44.

Stefan HG and Sinokrot BA. 1993. Projected global climate change impacts on water temperatures in five river central U.S. streams. *Climatic Change* **24**: 353-381.

Sinokrot BA, Stefan HG, McCormick JH and Eaton JG. 1995. Modeling of climate change on stream temperature and fish habitats below dams and near groundwater inputs. *Climatic Change* **30**: 181-200.

Todd DK. 1980. *Groundwater Hydrology*. Wiley: New York.

Tzeng, C. S., 1997. Studies on the population ecology of the Formosan landlocked salmon *Oncorhynchus masou formosanus* and evaluation of the hatchery ground. Construction and Planning Agency, Ministry of Interior, SHEI-PA National Park Management Office.

Tzeng, C. S., 1999. Studies on population ecology of the Formosan landlocked salmon *Oncorhynchus masou formosanus* (Ⅱ). Construction and Planning Agency, Ministry of Interior, SHEI-PA National Park Management Office.

Tung CP. 1995. *The Impacts of Land Use and Climate Changes on Streamflows and Corn Grain Yields and the Effects of Corn Production Response Strategies*. Ph.D. Dissertation, Cornell University. Ithaca: New York.

Tung CP and Haith DA. 1995. Global warming effects on New York streamflows. *Journal of Water Resources Planning and Management* **121**(2): 216-225.

Tung CP and Lee TY. 2001. Climate change impact assessment of the ChiChiaWan Creek streamflow. *Chinese Journal of Agricultural Engineering* **47**(1): 65-74.

Webb BW and Zhang Y. 1999. Water temperature and heat budgets in Dorset Chalk Water Courses. *Hydrological Processes* **13(3)**: 309-312.

Yang, C. H., 1997. *The Effect of the Water Temperature on Taiwan Landlocked Salmon (Oncorhynchus masou formosanus) in Chichiawan Stream Basin*. The Graduated Thesis of Graduate School of Life Science, National Tsing Hua University. (In Chinese)

Yogeh J and Kenneth ET. 1986. *Computational Heat Transfer*. Hemisphere Publishing Corporation: Washington, D.C.